PAPER

Single crystalline β-SiAlON nanowhiskers: preparation and enhanced properties at high temperature

Xinmei Hou,*[a] Ziyou Yu,[a] Zhiyuan Chen,[a] Baojun Zhao[b] and Kuo-Chih Chou[a]

Single crystalline β-SiAlON ($z = 1.0$) nanowhiskers with uniform morphology were prepared using a reaction sintering method at 1773 K for 6 h under flowing nitrogen atmosphere. The as-synthesized whiskers were well-crystallized with about 100–200 nm in diameter and a few hundred microns in length. According to the thermodynamic calculation, Al(g) and SiO(g) are important intermediate reactants to synthesize β-SiAlON whiskers. In the experiment, the two phases was controlled by changing the flow rate of nitrogen to make β-SiAlON whiskers grow in a stable way. The formation of β-SiAlON whiskers occurred through a vapor–solid (VS) mechanism. SiAlON was found to grow as a single crystal whisker from the $(10\bar{1}0)$ plane of the granule. Furthermore, an enhanced oxidation resistance for β-SiAlON whiskers at high temperature was also observed using the thermogravimetry method (TG), demonstrating that β-SiAlON whiskers with uniform morphology is a promising candidate as a reinforcing agent in composite.

1. Introduction

Ever since the discovery of carbon nanotubes by Iijima,[1] there has been great interest in the synthesis and characterization of one-dimensional (1D) structures due to their near-perfect crystalline nature, near-theoretical value of strength and unique physical and chemical performance.[2] β-SiAlON is one of the most common phases of SiAlON. It has a chemical formula of $Si_{6-z}Al_zO_zN_{8-z}$ ($z = 0$–4.2) with a hexagonal crystal structure.[3,4] Because of its characteristic structure, β-SiAlON crystal is usually developed into elongated prisms offering relatively high-fracture toughness. Moreover, the amount of Al in β-SiAlON can be adjusted to fit for various electrical applications. These properties enable elongated β-SiAlON materials to be a popular reinforcing and toughening agent in composites.[5,6]

Studies on elongated β-SiAlON material have remained very active ever since Lee and Cutler have done a pioneering work on the formation of SiC from rice husks.[7] Despite the volume of research and development (R&D) work going on at present,[7–14] progress in practical elongated β-SiAlON is still elusive. An utmost problem impeding the application of elongated SiAlON is how to prepare them with a uniform morphology, which is very important for engineering the properties of β-SiAlON-containing composite materials or a device for practical application. Recently, there has been a growing interest in the fabrication of β-SiAlON whiskers using various methods,[7–14] *e.g.* combustion

synthesis,[11] reaction sintering using pyrophyllite and resin or powder mixture of Al, Si and SiO_2 as raw materials.[12] By comparison, reaction sintering of the Al, Si and SiO_2 mixture is a much more efficient method to manipulate the morphology of β-SiAlON whiskers by controlling the processing parameters, such as temperature, partial pressure, flow rate of the gas phases, *etc.*[12–14] To our knowledge, there are few reports on the preparation of β-SiAlON whiskers with uniform morphology. The development of controlled experimental parameters to produce β-SiAlON whiskers with uniform morphology still remains a vital challenge in material chemistry.

In the present work, β-SiAlON whiskers with uniform morphology were prepared from a mixture of Si, Al and Al_2O_3 in flowing nitrogen. The suitable synthesis conditions were discussed from thermodynamic analysis and experimental result. The phase composition and morphology of β-SiAlON whiskers were characterized using X-ray diffraction (XRD), field emission scanning electron microscopy (FE-SEM), transmission electron microscopy (TEM) and high-resolution electron microscopy (HREM). Based on this, the corresponding growth mechanism will be proposed briefly. The thermal behavior of β-SiAlON whiskers in air at high temperature was measured using thermogravimetry (TG).

2. Experimental procedure

β-SiAlON whiskers were synthesized in a vertical tube furnace under controlled atmosphere. Si (≥99.0%, 7.4 μm), Al (≥99.5%, 7.4 μm) and Al_2O_3 (≥99.5%, 5 μm) were used as raw materials and mixed for 10 h using absolute ethyl alcohol as the medium according to the stoichiometric composition of $Si_{4.4}Al_{1.6}O_{1.6}N_{6.4}$

[a]*State Key Laboratory of Advanced Metallurgy, University of Science and Technology Beijing, Beijing100083, China.*
E-mail: houxinmei@ustb.edu.cn
[b]*Pyrometallurgy Research Centre, School of Chemical Engineering, The University of Queensland, Brisbane, Qld 4072, Australia*

($z = 1.6$). Pellets of solid samples were made with a die and a hydraulic press. The pellets were placed into an alumina crucible together with β-Si_3N_4 powder and then sintered at 1773 K for 6 h. High purity nitrogen gas (≥99.999%) was introduced into the alumina reaction tube at a rate range from 0.4–0.6 L min^{-1} and its pressure was maintained at 0.1 MPa.

The phases were identified by X-ray diffraction (XRD; M21XVHF22, MAC Science, Yokohama, Japan) using Cu Kα radiation in the angular 10–80°. The morphology and composition of the whiskers were examined by thermal field emission scanning electron microscopy (FE-SEM; ZEISS SUPRATM 55, Germany) and transmission electron microscopy (TEM, HITACHI H8100, Hitachi, Japan). High resolution electron microscopy (HRTEM, JEM 2010, Joel Ltd, Japan) operating at 200 kV was used to characterize the phase and crystal morphology of the products. The oxidation resistance of β-SiAlON whiskers (about 3.650 mg sample) was examined up to 1773 K in air at a heating rate of 10 K min^{-1} using a thermoanalyser (Netzsch STA449C). The sensitivity of the TG microbalance is ±0.0001 mg, which makes it possible to record accurate weight changes during the oxidation.

3. Thermodynamic calculation

Two systems, Si–O–N and Al–O–N, were involved during the formation of β-SiAlON whiskers. In the experiment, high purity nitrogen gas (≥99.999%) was used and its pressure was kept at 0.1 MPa. Thus the pressure of N_2, i.e. $P_{N_2}/P^\theta \approx 1$. In the following section, the possible reactions involved and the underlying thermodynamic principle will be discussed.

3.1 Si–O–N system

Since β-Si_3N_4 powder in the experiment is employed to control the reaction atmosphere,[13,14] the possible solid phases in the system are β-Si_3N_4, Si_2N_2O and SiO_2. The reactions between the solid phases and O_2 contained in N_2 atmosphere are following:

$$2Si_3N_4(s) + 1.5O_2(g) = 3Si_2N_2O(s) + N_2(g) \quad (1)$$
$$\Delta_rG(P,T) = -1\,005\,973 - 25\,T + 8.314 \ln 10\,T[\lg(P_{N_2}/P^\theta) - 1.5\lg(P_{O_2}/P^\theta)](J\,mol^{-1})$$

From the above equation, it can be seen that the reaction Gibbs free energy, Δ_rG is the function of temperature T and the partial pressure of gas phases, P_{N_2} and P_{O_2}. Therefore, eqn (1) can reach thermodynamic equilibrium at the experimental temperature (about 1800 K) by adjusting the partial pressure of the gas phases, i.e. $\Delta_rG(P,T) = 0$. Based on this, the relationship between the reaction equilibrium constant of eqn (1) and the partial pressure of the gas phases at 1800 K can be calculated as following:

$$\lg K_{1800\,K} = (1\,005\,973 + 25 \times 1800)/(19.13 \times 1800)$$
$$= \lg(P_{N_2}/P^\theta) - 1.5\lg(P_{O_2}/P^\theta) = 30.52$$

Similarly, the relationship between the reaction equilibrium constant and P_{N_2} and P_{O_2} of the following reaction can also be calculated.
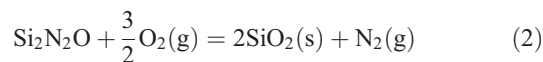
$$Si_2N_2O + \frac{3}{2}O_2(g) = 2SiO_2(s) + N_2(g) \quad (2)$$
$$\Delta_rG(P,T) = -941\,049 + 104.28\,T$$
$$+ 8.314 \ln 10\,T[\lg(P_{N_2}/P^\theta) - 1.5\lg(P_{O_2}/P^\theta)]$$
$$\times (J\,mol^{-1})\,\lg K_{1800\,K}$$
$$= \lg(P_{N_2}/P^\theta) - 1.5\lg(P_{O_2}/P^\theta) = 21.86$$

In the Si–O–N system, Si-containing gases are Si(g), SiO(g), Si_2(g) and Si_3(g). The related reactions and constants are shown in Table 1.

According to the above equations, the equilibrium partial pressure of Si-containing gases in Si–O–N system at 1800 K as a function of oxygen and nitrogen partial pressure can be shown in Fig. 1. It can be seen that the partial pressure of SiO(g) is always higher than other gases in the range of the oxygen partial pressure investigated. In the experiment, β-Si_3N_4 powder was applied and the oxygen partial pressure is approximately 10^{-20} atm in the experimental temperature range. Therefore, SiO(g) is an important intermediate reactant during the synthesis of β-SiAlON whiskers. From the above equations, SiO can be formed by oxidization of β-Si_3N_4, which further confirmed the role of β-Si_3N_4 powder used in the experiment from thermodynamic viewpoint. This is in agreement with the result reported in the literature.[16,17]

3.2 Al–O–N system

In view of Al–O–N system, the possible solid phases in the reaction are AlN, Al_3O_3N spinel phase[18] and Al_2O_3. The reaction between AlN and O_2 is:

$$2AlN(s) + 1.5O_2(g) = Al_2O_3(s) + N_2(g) \quad (15)$$
$$\Delta G_r(P,T) = -1\,028\,700 + 92.2\,T + 8.314 \times \ln 10$$
$$\times T[\lg(P_{N_2}/P^\theta) - 1.5\lg(P_{O_2}/P^\theta)]$$

when eqn (15) reaches thermodynamic equilibrium at the experimental temperature, i.e. 1800 K or so. The relationship between the reaction equilibrium constant and the partial pressure of the gas phases can be expressed as following:
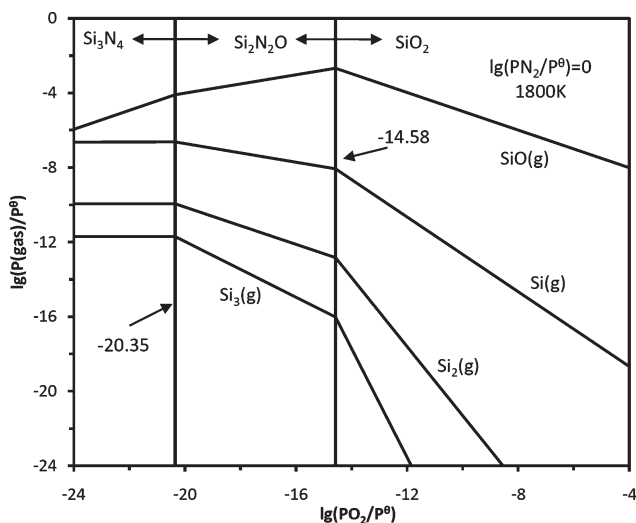
$$\lg K_{1800\,K} = \lg(P_{N_2}/P^\theta) - 1.5\lg(P_{O_2}/P^\theta) = 28.48$$

In Al–O–N system, Al-containing gases are Al(g), Al_2O(g), AlO(g), Al_2O_2(g) and AlO_2(g). In an analogous way, the related reaction equilibrium constants and the thermodynamic data of the reactions involved between the solid phases and the gaseous phases are calculated as shown in Table 2.

According to the above equations and thermodynamic data, the equilibrium partial pressure of Al-containing gases in Al–O–N system at 1800 K as a function of oxygen and nitrogen partial pressure is shown in Fig. 2. From Fig. 2, it can be seen

Table 1 The reactions and related thermodynamic data in Si–O–N system at 1800 K[15]

Equations	The reaction constants at 1800 K
$Si_3N_4(s) = 3Si(g) + 2N_2(g)$ (3)	$2 \lg(P_{N_2}/P^\theta) + 3 \lg(P_{Si(g)}/P^\theta) = -19.93$
$Si_3N_4(s) + \frac{3}{2}O_2(g) = 3SiO(g) + 2N_2(g)$ (4)	$2 \lg(P_{N_2}/P^\theta) + 3 \lg(P_{SiO(g)}/P^\theta) - 1.5 \lg(P_{O_2}/P^\theta) = 18.16$
$Si_3N_4(s) = \frac{3}{2}Si_2(g) + 2N_2(g)$ (5)	$2 \lg(P_{N_2}/P^\theta) + 1.5 \lg(P_{Si_2}(g)/P^\theta) = -14.94$
$Si_3N_4(s) = Si_3(g) + 2N_2(g)$ (6)	$2 \lg(P_{N_2}/P^\theta) + \lg(P_{Si_3}(g)/P^\theta) = -11.71$
$Si_2N_2O(s) + \frac{1}{2}O_2(g) = 2SiO(g) + N_2(g)$ (7)	$\lg(P_{N_2}/P^\theta) + 2 \lg(P_{SiO(g)}/P^\theta) - 0.5 \lg(P_{O_2}/P^\theta) = 1.94$
$Si_2N_2O(s) = 2Si(g) + \frac{1}{2}O_2(g) + N_2(g)$ (8)	$\lg(P_{N_2}/P^\theta) + 2 \lg(P_{Si(g)}/P^\theta) + 0.5 \lg(P_{O_2}/P^\theta) = -23.45$
$Si_2N_2O(s) = Si_2(g) + \frac{1}{2}O_2(g) + N_2(g)$ (9)	$\lg(P_{N_2}/P^\theta) + \lg(P_{Si_2(g)}/P^\theta) + 0.5 \lg(P_{O_2}/P^\theta) = -20.13$
$Si_2N_2O(s) = \frac{2}{3}Si_3(g) + \frac{1}{2}O_2(g) + N_2(g)$ (10)	$\lg(P_{N_2}/P^\theta) + \frac{2}{3}\lg(P_{Si_3(g)}/P^\theta) + \frac{1}{2}\lg(P_{O_2}/P^\theta) = -17.97$
$SiO_2(s) = SiO(g) + \frac{1}{2}O_2(g)$ (11)	$\lg(P_{SiO}/P^\theta) + 0.5 \lg(P_{O_2}/P^\theta) = -10.01$
$SiO_2(s) = Si(g) + O_2(g)$ (12)	$\lg(P_{Si}/P^\theta) + \lg(P_{O_2}/P^\theta) = -22.68$
$SiO_2(s) = \frac{1}{2}Si_2(g) + O_2(g)$ (13)	$0.5 \lg(P_{Si_2}/P^\theta) + \lg(P_{O_2}/P^\theta) = -20.21$
$SiO_2(s) = \frac{1}{3}Si_3(g) + O_2(g)$ (14)	$\frac{1}{3}\lg(P_{Si_3}/P^\theta) + \lg(P_{O_2}/P^\theta) = -19.64$

Fig. 1 Equilibrium partial pressure of gases in Si–O–N system at 1800 K.

powder to provide the SiO phase and control the oxygen partial pressure at the same time; (3) adjusting the flow rate of nitrogen: the flow rate was kept at 0.6 L min^{-1} before heating to 1773 K. It was slowed down to 0.4 L min^{-1} at 1773 K and kept at 0.5 L min^{-1} when cooling down to room temperature.

4. Results and discussion

4.1 Phase analysis

Fig. 3 shows the XRD patterns of the synthesized β-SiAlON prepared at 1773 K for 6 h. The identified spectra show that β-SiAlON was the main phase present. The diffraction pattern is in agreement with the data reported by the JCPDS (48-1615) card, *i.e.* z = 1.0, which was lower than that of the nominal starting composition, *i.e.* z = 1.6.

4.2 Morphology and microstructure observation

White wool-like materials were formed on the surface of the pellet. Fig. 4 shows the microstructure of synthesized β-SiAlON at different magnifications. It can be seen that the synthesized β-SiAlON is whiskers-like at lower magnification (Fig. 4a), while at higher magnification they have the shape of a belt from a strict viewpoint (shown in Fig. 4b and c). The morphology of β-SiAlON whiskers was uniform with about 100–200 nm in diameter and a few hundred microns in length. Fig. 4d shows a typical EDS spectrum for the β-SiAlON belt, showing the presence of Si, Al, O and N elements. From EDS results, the average molar ratio of Al/Si was estimated to be 0.23 and thus the z value was calculated to be 1.11, verifying the XRD analysis
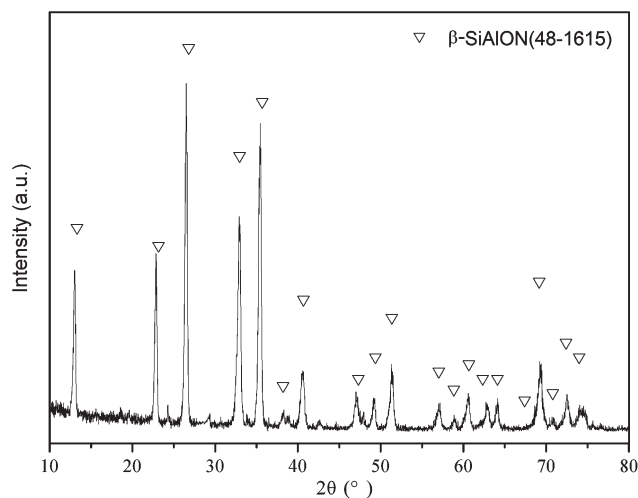
that the partial pressure of Al(g) is relatively higher than other gases at $P_{O_2} = 10^{-20}$ atm.

The above thermodynamic calculation indicates that Al and SiO may be important intermediate reactants during the synthesis of β-SiAlON whiskers at the experimental temperature range. Considering the gas phases play an important role during synthesis, the following three measurements have been adopted to enable β-SiAlON whiskers to grow in a stable way: (1) using a pellet of a Si, Al and Al$_2$O$_3$ solid sample to make β-SiAlON whiskers grow on the surface of the pellet; (2) using β-Si$_3$N$_4$

Table 2 The reactions and related thermodynamic data in Al–O–N system at 1800 K[15,18]

Equations		The reaction constants at 1800 K
$AlN(s) = Al(g) + 0.5N_2(g)$	(16)	$0.5 \lg(P_{N_2}/P^\theta) + \lg(P_{Al(g)}/P^\theta) = -4.2$
$AlN(s) + 0.25O_2(g) = 0.5Al_2O(g) + 0.5N_2(g)$	(17)	$0.5 \lg(P_{N_2}/P^\theta) + 0.5 \lg(P_{Al_2O(g)}/P^\theta) - 0.25 \lg(P_{O_2}/P^\theta) = -0.12$
$AlN(s) + 0.5O_2(g) = AlO(g) + 0.5N_2(g)$	(18)	$0.5 \lg(P_{N_2}/P^\theta) + \lg(P_{AlO(g)}/P^\theta) - 0.5 \lg(P_{O_2}/P^\theta) = 2.8$
$AlN(s) + 0.5O_2(g) = 0.5Al_2O_2(g) + 0.5N_2(g)$	(19)	$0.5 \lg(P_{N_2}/P^\theta) + 0.5 \lg(P_{Al_2O_2(g)}/P^\theta) - 0.5 \lg(P_{O_2}/P^\theta) = 2.45$
$AlN(s) + O_2(g) = AlO_2(g) + 0.5N_2(g)$	(20)	$0.5 \lg(P_{N_2}/P^\theta) + \lg(P_{AlO_2(g)}/P^\theta) - \lg(P_{O_2}/P^\theta) = 1.79$
$Al_3O_3N(s) = 3Al(g) + 1.5O_2(g) + 0.5N_2(g)$	(21)	$0.5 \lg(P_{O_2}/P^\theta) + \lg(P_{Al(g)}/P^\theta) = -14$
$Al_3O_3N(s) = 3AlO(g) + 0.5N_2(g)$	(22)	$0.5 \lg(P_{N_2}/P^\theta) + 3 \lg(P_{AlO(g)}/P^\theta) = -21$
$Al_3O_3N(s) = 1.5Al_2O(g) + 0.75O_2(g) + 0.5N_2(g)$	(23)	$0.75 \lg(P_{O_2}/P^\theta) + 1.5 \lg(P_{Al_2O}/P^\theta) + 0.5 \lg(P_{N_2}/P^\theta) = -29.76$
$Al_3O_3N(s) + 1.5O_2(g) = 3AlO_2(g) + 0.5N_2(g)$	(24)	$\lg(P_{AlO_2(g)}/P^\theta) - 0.5 \lg(P_{O_2}/P^\theta) = -8.01$
$Al_2O_3(s) = 2Al(g) + 1.5O_2(g)$	(25)	$2 \lg(P_{Al(g)}/P^\theta) + 1.5 \lg(P_{O_2}/P^\theta) = -36.34$
$Al_2O_3(s) = Al_2O(g) + O_2(g)$	(26)	$\lg(P_{Al_2O(g)}/P^\theta) + \lg(P_{O_2}/P^\theta) = -28.18$
$Al_2O_3(s) = 2AlO(g) + 0.5O_2(g)$	(27)	$2 \lg(P_{AlO(g)}/p^\theta) + 0.5 \lg(P_{O_2}/P^\theta) = -22.34$
$Al_2O_3(s) = Al_2O_2(g) + 0.5O_2(g)$	(28)	$\lg(P_{Al_2O_2(g)}/P^\theta) + 0.5 \lg(P_{O_2}/P^\theta) = -23.04$
$Al_2O_3(s) + 0.5O_2(g) = 2AlO_2(g)$	(29)	$2 \lg(P_{AlO_2(g)}/P^\theta) - 0.5 \lg(P_{O_2}/P^\theta) = -24.36$
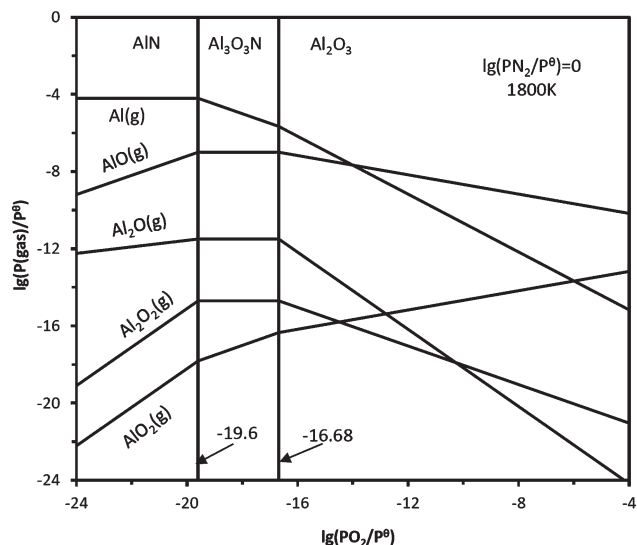
Fig. 2 Equilibrium partial pressure of gases in Al–O–N system at 1800 K.

Fig. 3 XRD pattern of β-SiAlON whiskers ($z = 1.1$) synthesized at 1773 K for 6 h.

result. The z value of β-SiAlON synthesized in the experiment was lower than that of the nominal starting composition. The main reason was probably that SiO from Si_3N_4 powder can increase the SiO ratio and thus the z value of the obtained SiAlON decreased.

TEM micrograph of β-SiAlON whiskers together with the result of the selected area electron diffraction (SAED) is shown in Fig. 5a. The diffraction patterns (inset of Fig. 5a) indicate that the β-SiAlON whisker is a single crystal and grows along the c-axis. HREM was also employed to analyze the structure of the single crystal and the result is shown in Fig. 5b. The lattice image indicates that the plane distance of a single β-SiAlON is about 0.660 nm, which is close to the ($10\bar{1}0$) lattice spacing of β-SiAlON (0.661 nm, PDF card No. 48-1615).

4.3 Mechanism of whisker growth

VS (Vapor–solid) and VLS (vapor–liquid–solid) are two well known mechanisms for the formation of whiskers.[19] In the VLS mechanism a liquid droplet will be initially formed, and then reactant molecules in the vapor are transported by diffusion to the liquid–solid interface, where precipitation occurs and with crystal growth the droplet is detached from the substrate. During the cooling stage the liquid droplet forms a nodule at the top of the whisker, which is considered a characteristic morphology of the VLS mechanism. In the micrographs of the β-SiAlON whiskers observed in this study, no nodule was observed at the ends of those whiskers. As shown in Fig. 5a, the top of the belts is well developed, indicating that β-SiAlON whiskers were mainly nucleated by the VS mechanism.[11,20] The growth schematic diagram of β-SiAlON whiskers is illustrated in Fig. 6. At the beginning of the reaction, β-Si_3N_4 powder used in the
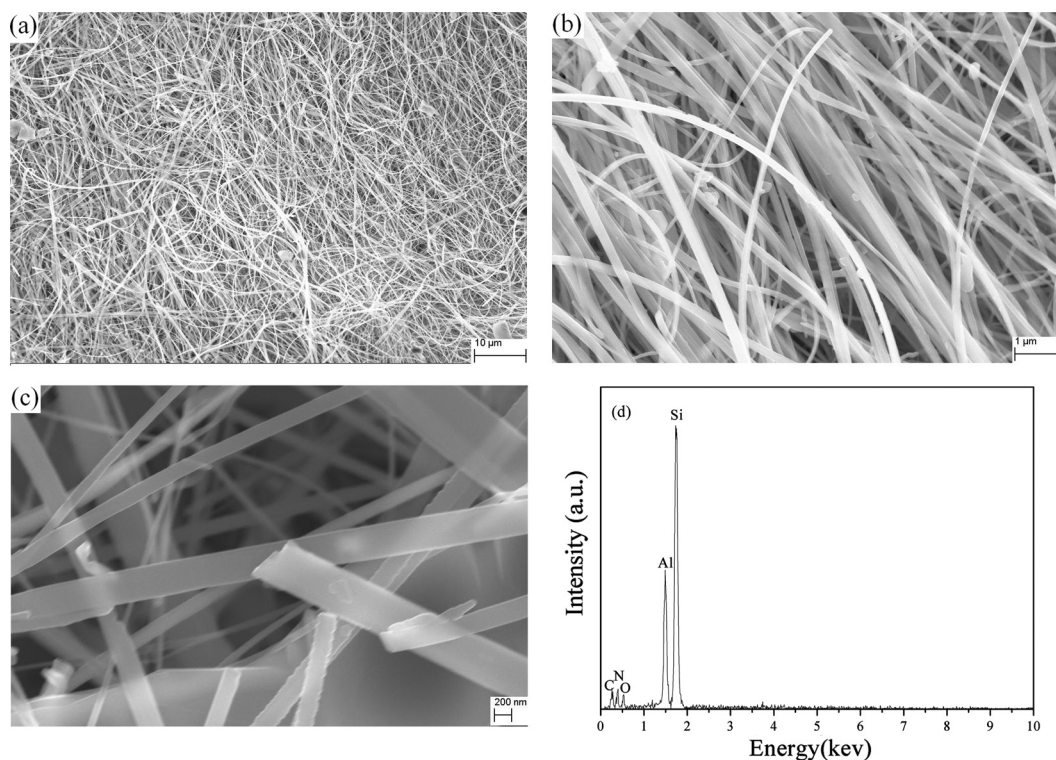
Fig. 4 (a–c) SEM micrograph at different magnifications and (d) EDS spectrum of β-SiAlON whiskers.

experiment promoted the formation of β-SiAlON nuclei in flowing nitrogen.[16,17] The β-SiAlON formed on the surface of the pellet acts as crystal seeds. These β-SiAlON nuclei accelerated the growth of whiskers (Fig. 6a). It is believed that at the beginning of the nucleation/growth of β-SiAlON nuclei, the growth of the nuclei occurs along all directions simultaneously. However, the growth rate along the width direction, *i.e.* (10$\bar{1}$0) plane, was much greater due to the anisotropy nature of β-SiAlON crystal structure (Fig. 6b). The anisotropic grain growth is a common phenomenon in β-SiAlON[11,21] and has also been proven in the experimental result, as shown in the right part of Fig. 6b, which was the microstructure of β-SiAlON synthesized at 1773 K for 3 h. It can be seen that β-SiAlON whiskers grew along their longitudinal directions. Thus these new β-SiAlON synthesized from SiO, AlN and Si_3N_4 in flowing nitrogen gas deposited on the preferential growth plane of the β-SiAlON seeds, (10$\bar{1}$0) plane (Fig. 6b). With the continuous cycle, the β-SiAlON whiskers with uniform morphology were finally formed (Fig. 6c). This is consistent with the work on the growth of platelike and branched Si_3N_4 whiskers.[22] Further experiments would be required to confirm the theory.

4.4 Oxidation resistance

Fig. 7 shows the non-isothermal oxidation behavior of β-SiAlON whiskers. For comparison, the oxidation of the β-SiAlON whiskers (z = 1.1) with non-uniform morphology *i.e.* the diameter range from 80–600 nm, was also investigated (curve a). It can be seen from Fig. 7 that β-SiAlON whiskers with uniform morphology (curve b) exhibited better oxidation resistance. Its

oxidation reaction started at 1300 K and the reaction rate increased rapidly between 1300 and 1500 K. The oxidation rate leveled off from 1500 K and increased again from 1700 K. The total mass of the β-SiAlON whiskers with uniform morphology was found to have increased by 3.85%, which was much lower than that of β-SiAlON whiskers with non-uniform morphology, 9.75%.

The main reason that caused the different oxidation behavior of the above β-SiAlON whiskers was the shape of the sample, which can be explained by Chou's model.[14,23] According to Chou's model, the oxidation behavior of non-oxide materials belonged to the gas–solid reaction and was affected by many factors including the shape of the sample. The oxidation behaviour can be expressed as following:

$$\xi = 1 - \left[1 - \frac{1}{R_0} \sqrt{ \frac{ 2D_O^0 k_O^0 \left(\sqrt{P_{O_2}} - \sqrt{P_{O_2}^{eq}} \right) }{ v_m \exp(\Delta E_d / RT) } t } \right]^2 \quad (30)$$

where ξ represents the oxidation fraction; ΔE_d the apparent activation energy of diffusion; P_{O_2} the oxygen partial pressure above the surface of the sample, $P_{O_2}^{eq}$ the oxygen partial pressure in equilibrium with oxide in oxide–SiAlON interface, which is related to the temperature T. Both k_O^0 and D_O^0 are constants independent of temperature T but relying on the materials; v_m is a coefficient that depends on the sample and reaction; R_0 is the diameter of the β-SiAlON whisker.

For β-SiAlON whiskers with non-uniform morphology, the value of R_0 varied from 80–600 nm and the percentage of β-SiAlON whiskers with a smaller diameter, R_0 amounted to

50%.[14] By comparison, the value of R_0 of β-SiAlON whiskers with uniform morphology was in the range of 100 nm. According to eqn (30), β-SiAlON whiskers with non-uniform morphology were easy to be oxidized and had a larger reaction fraction.

5. Conclusions

Si, Al and Al_2O_3 were used as raw materials to synthesize β-SiAlON nanowhiskers with uniform morphology in flowing nitrogen atmosphere. Thermodynamic calculations show that Al (g) and SiO(g) could be essential intermediate reactants for synthesizing β-SiAlON whiskers.
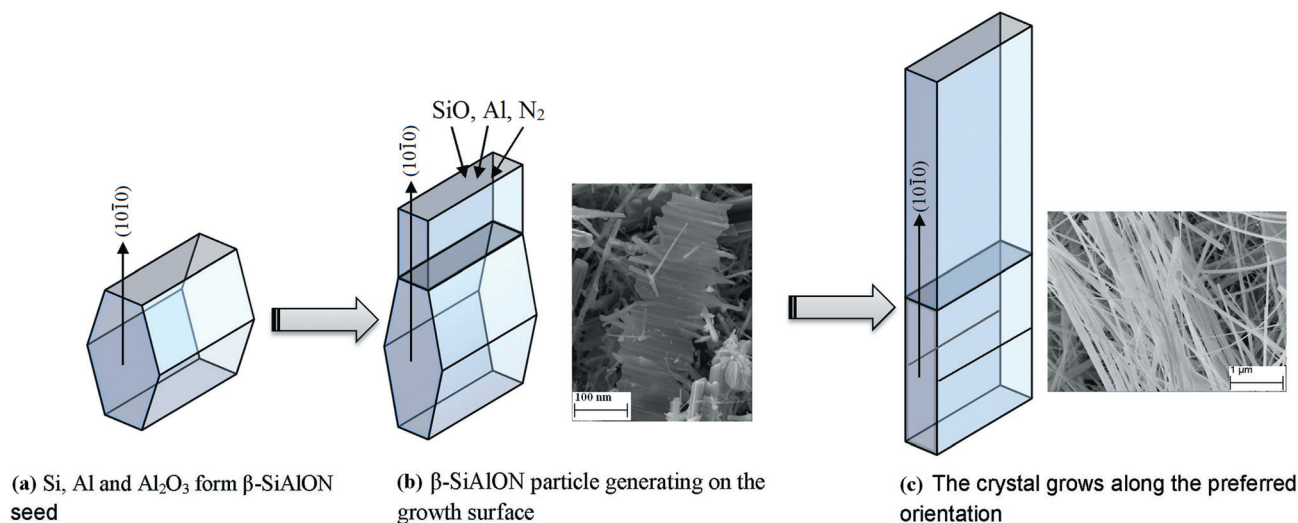
β-SiAlON nanowhiskers with uniform morphology were produced by the reaction sintering method at 1773 K for 6 h in flowing nitrogen atmosphere. The diameters of the whiskers were about 100–200 nm and their length extended to a few hundred microns. The growth of the whiskers was controlled by a VS mechanism. At the beginning of the reaction, β-Si_3N_4 powder used in the experiment promoted the formation of β-SiAlON nuclei in flowing nitrogen. The vapor phase, SiO
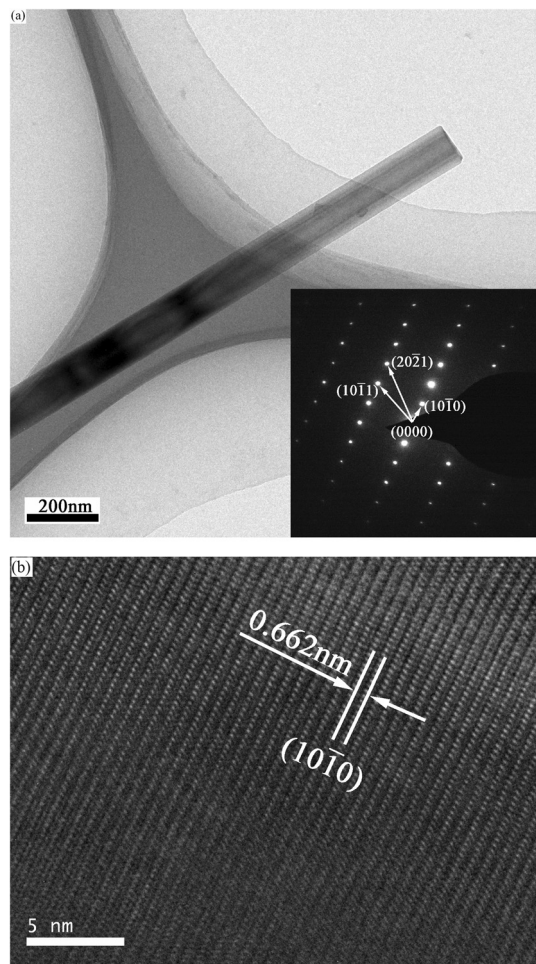
Fig. 5 TEM results of a β-SiAlON whisker: (a) TEM image with SEAD pattern; (b) HRTEM image of the whisker's head.
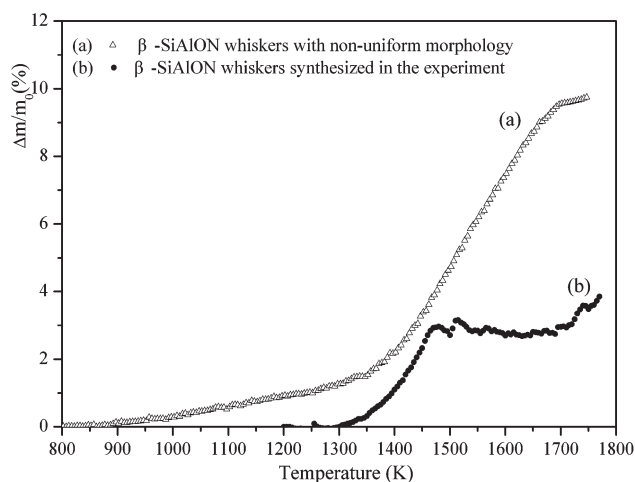
Fig. 7 Comparison of non-isothermal oxidation behaviour of β-SiAlON whiskers with non-uniform morphology (a) and uniform morphology (b) at a heating rate of 10 K min^{-1}.

(a) Si, Al and Al_2O_3 form β-SiAlON seed

(b) β-SiAlON particle generating on the growth surface

(c) The crystal grows along the preferred orientation

Fig. 6 Schematic diagram of the growth mechanism of β-SiAlON whiskers.

reacted with AlN and Si_3N_4 to form β-SiAlON and was deposited on the preferential growth plane of β-SiAlON seeds, *i.e.* (10$\bar{1}$0). With the continuous cycle, the β-SiAlON whiskers with uniform morphology were finally formed. Furthermore, the oxidation resistance of β-SiAlON nanowhiskers was found to be improved.

Acknowledgements

References

1 S. Iijima, *Nature*, 1991, **354**, 56A.
2 J. S. Pan, R. X. Cao and Y. W. Yuan, *Mater. Lett.*, 2006, **60**, 626.
3 Y. Oyama and O. Kamigaito, *Jpn. J. Appl. Phys.*, 1971, **10**, 1637.
4 K. H. Jack and W. I. Wilson, *Nature (London) Phys. Sci.*, 1972, **238**, 28.
5 Z. Shen, Z. Zhao, H. Peng and M. Nygren, *Nature*, 2002, **417**, 266.
6 I. W. Chen and A. Rosenflanz, *Nature*, 1997, **389**, 701.
7 Z. X. Chen, *J. Mater. Sci.*, 1993, **28**, 6021.
8 J. Yu, S. Ueno, K. Hiragushi, S. Zhang and A. Yamaguchi, *J. Ceram. Soc. Jpn.*, 1997, **105**, 821.
9 X. Jia, H. Zhang, J. Chen, D. Yang and Z. Liu, *J. Chin. Ceram. Soc.*, 2004, **32**, 925.
10 R. Fu, K. X. Chen and J. M. F. Ferreira, *Key Eng. Mater.*, 2005, **280–283**, 1241.
11 G. H. Liu, K. X. Chen, H. P. Zhou, K. G. Ren, J. T. Li, C. Pereira and J. M. F. Ferreira, *Scr. Mater.*, 2006, **55**, 935.
12 D. H. L. Ng, T. L. Y. Cheung, F. L. Kwong, Y. F. Li and R. Yang, *Mater. Lett.*, 2008, **62**, 1349.
13 P. L. Dong, X. D. Wang, M. Zhang, M. Guo and S. Seetharaman, *J. Nanomater.*, 2008, 1.
14 X. M. Hou, C. S. Yue, A. K. Singh, M. Zhang and K. C. Chou, *Corros. Sci.*, 2011, **53**, 2051.
15 M. W. Chase, Jr.*et al.*, in *JANAF Thermochemical Tables*, American Chemical Society and American Institute of Physics for NBS, New York, 3rd edn, 1985, p. 120.
16 A. D. Mazzoni and E. F. Aglietti, *Appl. Clay Sci.*, 1998, **12**, 447.
17 C. S. Yue, M. Guo, M. Zhang, X. D. Wang, Z. A. Zhang and B. Peng, *J. Chin. Inorg. Mater.*, 2009, **24**, 1163.
18 H. X. Willems, *J. Eur. Ceram. Soc.*, 1992, **10**, 339.
19 *Whisker Technology*, ed. A. P. Levitt, John Willey & Sons, New York, NY, 1970, p. 215.
20 M. Johnsson, *Solid State Ionics*, 2004, **172**, 365.
21 M. Kramer, D. Wittmuss, H. Kuppers, M. J. Hoffmann and G. Petzow, *J. Cryst. Growth*, 1994, **140**, 157.
22 W. Y. Yang, Z. P. Xie, J. J. Li, H. Z. Miao, L. G. Zhang and L. N. An, *Solid State Commun.*, 2004, **132**, 263.
23 K. C. Chou and X. M. Hou, *J. Am. Ceram. Soc.*, 2009, **92**, 585.